ELSEVIER

Catalysis Today 47 (1999) 161–167

CATALYSIS TODAY

The reduction and oxidation behaviour of manganese oxides

E.R. Stobbe*, B.A. de Boer, J.W. Geus

Department of Inorganic Chemistry, Debye Institute, Utrecht University, Sorbonnelaan 16, 3584 CA Utrecht, Netherlands

Abstract

The reduction of manganese oxides with methane was studied to investigate the suitability of manganese as an oxygen storage compound. Manganese oxides are reduced by CH_4 to a lower-valent manganese oxide, producing CO_2 and water. Once the manganese oxide is reduced, it can be regenerated, i.e. reoxidised. By integrating this exothermic oxidation cycle with endothermic methane reforming, a new setup for exothermic, small scale syngas production is obtained. Manganese oxides can be reduced to manganese(II) oxide with methane at temperatures higher than 723 K. Reoxidation of MnO at 823 K leads to the formation of Mn_2O_3 at 823 K. At 1073 K reoxidation of MnO gives Mn_3O_4 , which corresponds to a lower Mn-valency than expected thermodynamically. Subsequent oxidation–reduction cycles lead to an increase in reduction temperature, probably due to a higher crystallinity. © 1999 Elsevier Science B.V. All rights reserved.

Keywords: Manganese oxide (MnO_x); Methane; Oxidation

1. Introduction

Current processes for syngas production have several drawbacks. The most widely used process for syngas production, methane-steam reforming, has the disadvantage of NO_x formation, which is caused by burners used for this highly endothermic process. Moreover, expensive multitubular, high-temperature resistant reactors are used [1,2]. On the other hand, the partial oxidation of methane to synthesis gas is slightly exothermic. Unfortunately, direct catalytic partial oxidation is often thought to proceed through a two-step mechanism: Methane is oxidised exothermally to carbon dioxide and water, after which carbon monoxide and hydrogen are formed in subsequent endothermic reforming reactions [3,4]. The high temperature gradients, the risk of explosions and the need for pure oxygen are major drawbacks of this process.

A novel two-step process for the production of syngas out of methane and air has been proposed by Van Looij [3]. In this process methane is oxidised in the absence of gas-phase oxygen by a metal oxide, that acts as an oxygen storage compound (OSC). Once the storage capacity has been used, i.e. the metal oxide is reduced, the lower-valent oxide or metal is regenerated, i.e. re-oxidised, by air. By using two parallel reactors, one in which the OSC oxidises methane, and one in which the regeneration of the OSC proceeds, a continuous oxidation process can be obtained. Both heat and products, viz. CO_2 and H_2O, can be used for the subsequent endothermic production of syngas. Schematically the overall process is shown in Fig. 1.

This novel setup for the partial oxidation of methane to syngas, the integration of oxidation of methane by an OSC with a reforming reactor, has the advantage of being slightly exothermic, and of the absence of explosion risks, because gaseous oxidant

---

*Corresponding author. E-mail: e.r.stobbe@chem.uu.nl

PII: S0920-5861(98)00296-X

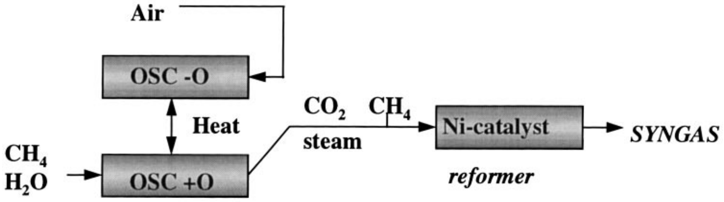

Fig. 1. A novel process for the production of syngas: (OSC+O=reoxidised/fresh, OSC−O=reduced/exhausted).

and fuel are separated. Moreover, air can be used instead of pure oxygen, which brings about considerable cost saving. Due to the relatively low operating temperature and the absence of burners, NO_x formation is prevented [3].

However, most transition metal oxides are not suitable for the oxidation of methane in the absence of oxygen. For instance, iron, cobalt and nickel, formed in the reduction, show the formation of carbides and carbon whiskers in the presence of methane [3,5]. Copper does not show carbon deposition, but shows a very high volatility [6]. Manganese oxides, however, are expected to exhibit a relatively low volatility. The reduction to a metallic phase, which is favourable for both sintering and carbide formation, is highly unlikely for manganese. We think that, among the transition metal oxides, manganese oxide is unique in this behaviour.

Manganese oxides are known to be active catalysts in several oxidation or reduction reactions. Manganese oxides can be used as catalysts for the oxidation of methane and carbon monoxide [7], or the selective reduction of nitrobenzene [8,9]. Moreover, the application of manganese oxides as an oxygen storage component (OSC) for a three-way catalyst has been proposed. Recently Chang and McCarty [10] showed oxygen absorption and desorption behaviour of manganese oxide to be superior to that of cerium oxide.

In all of these applications the redox properties of manganese oxide play a key role. The catalytic oxidation of methane over manganese oxide is supposed to proceed through a Mars and van Krevelen mechanism [7]. In the oxidation of methane lattice oxygen is consumed. Therefore, in principle, manganese oxide should be able to oxidise methane in the absence of gas-phase oxygen. Of the manganese oxides which are known, the most important phases and their transition temperatures in air are given in Fig. 2.

The reoxidation of manganese oxides is reversible up to Mn_2O_3, reoxidation to MnO_2 in pure oxygen only proceeds at pressures higher than 3000 bar. Van de Kleut [7] has shown that (supported) manganese catalysts can be reduced with methane at temperatures above 250°C. This temperature is far below the operating temperature of the oxidation of methane with the OSC, which will proceed at temperatures higher than the reformer unit, which usually operates at temperatures of about 1100 K.

The aim of this investigation is to get insight into the reduction behaviour of unsupported manganese oxides in the presence of methane. Also the reoxidation behaviour of manganese oxides is investigated. On the basis of both reduction and reoxidation an evaluation of the suitability of manganese oxides as an OSC for the cyclic oxidation of methane will be made. Only unsupported manganese oxides are involved in order to rule out support effects.

2. Experimental

2.1. Materials

For the preparation of the samples, mostly procedures according to Van de Kleut [7] were used. MnO_2 was prepared by calcining $Mn(NO_3)_2{\cdot}4H_2O$ (Merck

$$MnO_2 \xrightarrow{500^\circ C} Mn_2O_3 \xrightarrow{900^\circ C} Mn_3O_4 \xrightarrow{1700^\circ C} MnO$$

Fig. 2. The most common manganese oxide phases in air at different temperatures.

p.a.) in air for 13 h at 145°C. Mn_2O_3 was prepared by heating $MnCO_3{\cdot}xH_2O$ in air consecutively for 3 h at 120°C, 8 h at 240°C, and finally 8 h at 550°C. Mn_3O_4 was prepared by two different methods. A "high" surface area Mn_3O_4 was prepared by precipitation from a manganese nitrate solution with ammonia in a nitrogen atmosphere, and subsequent drying of the manganese hydroxide precipitate in air at 130°C for 72 h. A low surface area Mn_3O_4 was prepared by calcining $MnCO_3$ at 1000°C in air for 8 h.

2.2. Characterisation

The oxides were characterised at room temperature by X-ray diffraction on a Nonius PDS 120 powder diffractometer system, equipped with a position sensitive detector of 120°2θ. The radiation used was Cu K_{α_1}, λ=1.5406 Å.

The oxidation state of the samples, or manganese–oxygen ratio, was determined by temperature-programmed reduction with hydrogen on a conventional TPR flow apparatus equipped with a HWD. Samples of 30 mg were heated from room temperature to 1050 K in a mixture of 10% H_2 in Ar (50 ml/min), with a heating rate of 5 K/min. A cold trap was used for the removal of water. For the determination of the oxidation state of the samples, reduction not further than to MnO was assumed. Copper(II)oxide was used as a calibration compound.

The specific surface area of the samples was determined by the BET method using nitrogen adsorption–desorption isotherms (Micromeritics ASAP2400).

2.3. Temperature-programmed experiments

Temperature-programmed experiments were performed in an automated flow apparatus. Reductions were carried out in a mixture of 1% methane in argon. Methane consumption was always lower than 20%. The samples were (re-) oxidised in a mixture of 5% oxygen in Ar (100 ml/min). An amount of 80 mg sieve fraction (0.15–0.50 mm) of oxide was heated in 1% methane in argon from room temperature to 1100 K with a heating rate of 5 K/min. After 2 h of isothermal reduction at 1100 K, the sample was cooled down to 823 K in argon after which reoxidation in 5% oxygen in argon was performed isothermally for 2 h. Subsequently the sample was cooled down in 5% oxygen in argon to 473 K. After purging with argon a next reduction–reoxidation cycle was performed.

Products were analysed by an on-line gas chromatograph (Chrompack CP9001) equipped with two columns and two detectors. A permapure dryer was used for the removal of water. A Porapak column was used to separate carbon containing products, which were detected by a flame ionisation detector after methanising. Hydrogen and oxygen were separated on a Molsieve 5A column and detected by a thermal conductivity detector. An on-line quadrupole mass spectrometer (Balzers) was used for short-time analysis of reactants and products.

3. Results and discussion

3.1. Characterisation

X-ray diffraction was used to determine the bulk crystalline phases in the samples. The diffraction patterns of the various manganese samples are shown in Fig. 3. The diffraction patterns indicate that no other bulk crystalline phases than the predicted phases were present in the samples. The diffraction patterns of MnO_2 and Mn_2O_3 corresponded with β-MnO_2 (pyrolusite) and α-Mn_2O_3, respectively. The Mn_3O_4 samples showed both similar diffraction patterns, representing the diffraction pattern of α-Mn_3O_4, haus-

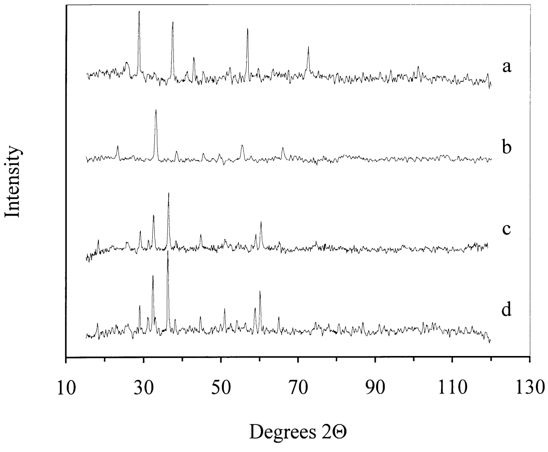

Fig. 3. XRD patterns of (a) MnO_2, (b) Mn_2O_3, (c) $Mn_3O_4^a$ and (d) $Mn_3O_4^b$.

Table 1
Characteristics of prepared manganese oxide samples

Sample	XRD	MnO_x ex TPR-H_2	Mn valency ex TPR-H_2	BET SA (m^2/g)
MnO_2	β-MnO_2 pyrolusite	$MnO_{1.96\pm0.03}$	3.92	0.3
Mn_2O_3	α-Mn_2O_3	$MnO_{1.48\pm0.03}$	2.96	26
$Mn_3O_4^a$	α-Mn_3O_4 hausmannite	$MnO_{1.31\pm0.03}$	2.62	8
$Mn_3O_4^b$	α-Mn_3O_4 hausmannite	$MnO_{1.33\pm0.03}$	2.66	1

mannite. The manganese oxide particles were too large to determine particle size by XRD. BET measurements, results of which are summarised in Table 1, showed a higher surface area for Mn_3O_4, which suggests a lower crystallinity. According to BET results, MnO_2 is the most crystalline phase, whereas Mn_2O_3 is the least crystallinic.

3.2. Temperature-programmed reduction with H_2

The oxygen-to-manganese ratios were determined by temperature-programmed reduction with hydrogen (Fig. 4). From the peak area, that was calibrated with the reduction of copper(II)oxide, the oxidation state of the manganese oxide samples was determined. The oxidation states of the samples were very close to the theoretical oxidation states. The oxidation states of the samples are shown in Table 1.

MnO_2 showed almost a one-step reduction, whereas Mn_2O_3 showed a clear two-step reduction. The peak areas of the latter correspond to subsequent reduction of Mn_2O_3 to Mn_3O_4 and MnO. The reduction of Mn_3O_4 in hydrogen is influenced by the preparation procedure.

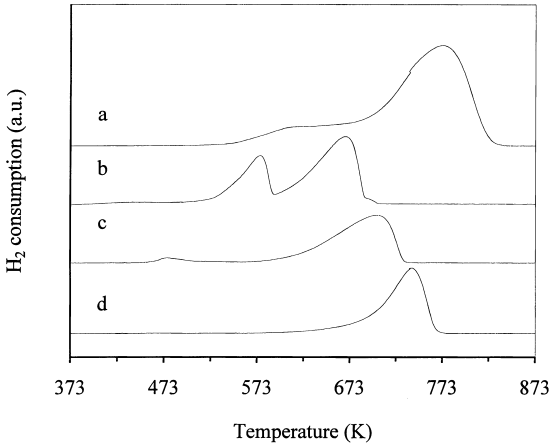

Fig. 4. Temperature-programmed reduction with hydrogen of (a) MnO_2, (b) Mn_2O_3, (c) $Mn_3O_4^a$ and (d) $Mn_3O_4^b$.

The more crystalline $Mn_3O_4^b$ reduces at higher temperatures and the nature of the oxygen is more uniform, which is indicated by the relatively narrow reduction peak. The small reduction peak at low temperature for the high surface $Mn_3O_4^a$ has been reported earlier [7]. Although found at somewhat higher temperature Weimin et al. [9] attributed this low temperature peak to the reduction of Mn(III) in tetrahedral sites.

The reduction profiles show that there is no direct correlation between the onset of reduction and the oxidation state of the samples. Mn_2O_3 exhibited the highest surface area and the lowest reduction temperature, whereas the low surface manganese oxides, MnO_2 and $Mn_3O_4^b$, exhibited the highest reduction temperatures. From this we can conclude that not the oxidation state, but the crystallinity or defect concentration determine the reducibility by hydrogen.

3.3. Temperature-programmed reduction with CH_4

The manganese oxide samples were reduced with methane to determine the oxygen storage capacity in the cyclic oxidation of methane. During the reduction of manganese oxide with methane, carbon dioxide and water were the main products. Carbon monoxide, hydrogen and higher hydrocarbons, viz. ethane and ethene, were produced only with insignificant yields (<1%).

The reduction profiles are shown in Fig. 5. All the samples showed quantitative reduction to MnO. After reduction with methane, the MnO_x stoichiometry was checked by TPR with H_2. TPR revealed a stoichiometry of $MnO_{1.00\pm0.01}$ for the samples. The formation

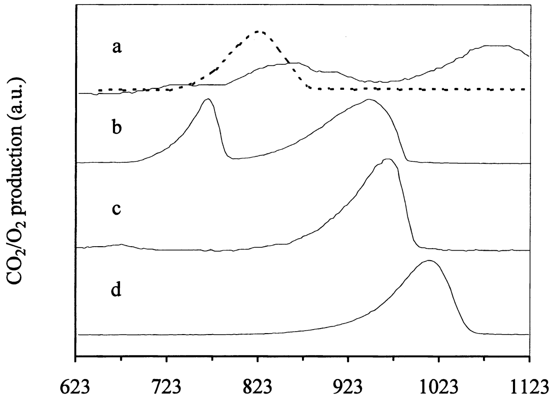

Fig. 5. Temperature-programmed reduction with methane of (a) MnO_2, (b) Mn_2O_3, (c) $Mn_3O_4^a$ and (d) $Mn_3O_4^b$. ((———) CO_2; (- - -) O_2 production).

of $MnO_{1.00}$ was confirmed by the green colour of the samples, which is typical for MnO.

MnO_2 showed a somewhat different behaviour than the other samples. The reduction of MnO_2 with methane, which is accompanied by the production of carbon dioxide and water, takes place simultaneously with the decomposition of MnO_2 into the lower-valent Mn_2O_3. The evolution of molecular oxygen, accompanying this decomposition, accounts for more than 75% of the reduction of MnO_2 to Mn_2O_3. This indicates that the desorption of oxygen is much faster than the oxidation of methane.

Heating of MnO_2 in inert, i.e. argon, results in a decomposition to Mn_2O_3 at the same temperature as reduction in CH_4. The further reduction of MnO_2 with methane proceeded at relatively high temperatures. Although not shown in Fig. 5, full reduction of MnO_2 to MnO could be accomplished at 1123 K.

As in the reduction with hydrogen, Mn_2O_3 showed a two-step reduction by methane to MnO via Mn_3O_4. Determination of the manganese valency by TPR (H_2) between the two reduction steps revealed a stoichiometry of $MnO_{1.33}$, which corresponds to Mn_3O_4.

In general it can be concluded that the trends in reducibility of manganese oxides with methane and hydrogen are the same. The oxide with the lowest crystallinity or the highest defect concentration is the easiest to reduce.

3.4. Reoxidation and multiple reduction–reoxidation cycles

In view of the utilisation of manganese oxide as an oxygen storage compound for the cyclic oxidation of methane, also its reoxidation behaviour is of great importance. Therefore we have investigated the influence of the reoxidation temperature and the influence of subsequent reduction–reoxidation cycles on the reduction behaviour. Reoxidation of the reduced samples was usually performed at 823 K, a temperature at which Mn_2O_3 is thermodynamically the most stable phase. For all reduced samples, reoxidation for 2 h at 823 K led to a manganese–oxygen stoichiometry of $MnO_{1.48\pm0.03}$, which corresponds to the expected formation of Mn_2O_3. Reoxidation at lower temperatures, viz. 673 K, was very slow. After 2 h of reoxidation at 673 K, formation of MnO to $MnO_{1.33}$, corresponding with Mn_3O_4, had been effectuated, whereas after 10 h $MnO_{1.50}$, corresponding with Mn_2O_3, had been formed. Obviously, Mn_2O_3 corresponds to the highest obtainable manganese valency, because further oxidation to MnO_2 can only be effectuated under extremely high oxygen pressures.

Reoxidation at higher temperatures, 1073 K, surprisingly, did not lead to a fast formation of the thermodynamically most stable Mn_2O_3. Even after 2 h, only the presence of Mn_3O_4 could be established.

A reoxidation temperature of 1073 K is close to the thermodynamical transition temperature of Mn_2O_3 to Mn_3O_4. Apparently, the thermodynamical driving force for oxidation to a higher manganese valency, which decreases at higher temperatures, is too small. In the cyclic reoxidation of methane, which will proceed at about 1100 K, apparently Mn_3O_4 will be formed in the regenerator unit, independent of the manganese valency of the fresh sample. Increasing the oxygen pressure or lowering the temperature of reoxidation could however result in the formation of Mn_2O_3.

The influence of the number of subsequent reduction–reoxidation cycles on the reducibility $Mn_3O_4^a$ is shown in Fig. 6. Subsequent temperature-programmed reduction with methane (up to 1123 K) and reoxidation (823 K) led to an increase in reduction temperature. The oxygen content of the regenerated samples remained constant (Mn_2O_3). The higher reduction temperatures must be due to a higher crystallinity, and this conclusion is supported by the fact

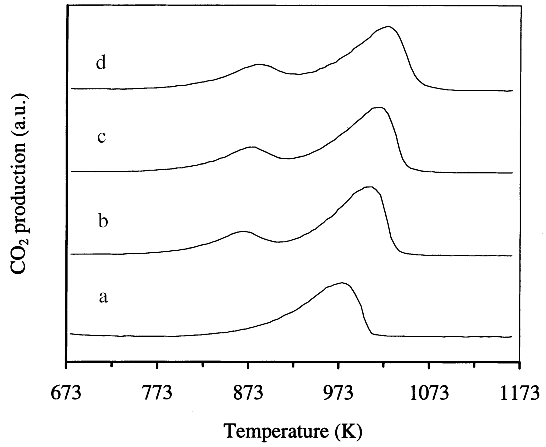

Fig. 6. The influence of subsequent reduction–reoxidation cycles on the reduction of $Mn_3O_4^a$ with methane reoxidation at 823 K.

that some sintering of the sieve fraction was observed. This ageing effect is not only important in the cyclic oxidation of methane, but could also be important for the application of manganese oxide as an oxygen storage compound for three-way catalysts. Possibly, this recrystallisation process and sintering can be prevented by using supported manganese oxides. The use of a thermostable support might influence the manganese oxide particle size and crystallinity, resulting in a decrease of the reduction temperature. On the other hand, a support could stabilise the manganese oxide, resulting in an increase in reducibility.

3.5. *Carbon deposition*

Carbon deposition during the reduction of manganese oxide with methane is highly undesired. Therefore we have investigated the carbon deposition activity of Mn_2O_3 and $Mn_3O_4^b$. The samples were reduced in a flow of 1% methane at 1100 K and kept at this temperature in methane for 20 h. After cooling down rapidly, temperature-programmed gasification of the carbon with oxygen revealed a total carbon deposition of 0.1 wt% on the low surface $Mn_3O_4^b$, and 0.2 wt% on the high surface Mn_2O_3 sample. These experiments show that only negligible carbon deposition had occurred.

However, carbon deposition might be more pronounced on high surface manganese oxides. The gasification results were confirmed by transmission electron microscopy (Philips CM200 and Philips EM420). With TEM analysis no graphitic or whisker-like carbon or any other form of carbon deposition was observed.

Moreover, we found that carbon deposition during reduction with methane at 1100 K can be prevented completely on all samples by adding 3% water to the feed (1% CH_4 balance Ar). Therefore the use of steam is two-fold; besides the use of steam for the heat integration of the process (Fig. 1), it will also be used to prevent carbon deposition.

4. Conclusions

Manganese oxides are capable of oxidising methane in the absence of gas-phase oxygen at temperatures higher than 723 K. The reduction rate of the manganese oxides is mainly determined by their crystallinity and not by their valency. This crystallinity is enhanced upon subsequent reduction and oxidation cycles, which results in a slower reduction of the manganese oxides by methane. This effect is not only important in the cyclic oxidation of methane, it is also important for it is an oxygen storage compound for three-way catalysts.

The reoxidation of MnO, which remains after the oxidation of methane, results in rapid formation of Mn_3O_4. At 1100 K no further oxidation of Mn_3O_4 takes place. At lower temperature further reoxidation to Mn_2O_3 can proceed. Under the expected process conditions, i.e. about 1200 K, of cyclic oxidation of methane as thermal energy source (and feed) for the methane reforming reactions, the following cycle will take place.

Mn_3O_4 will oxidise methane under the formation of water, carbon dioxide and MnO. Subsequently MnO will be regenerated, with air to Mn_3O_4. Only negligible carbon deposition was observed. This carbon laydown can be prevented completely by adding small amounts of water to the feed.

Acknowledgements

The authors would like to thank Gastec N.V. for the financial support to this research.

References

[1] J.R. Rostrup-Nielsen, Catal. Today 18 (1993) 305.
[2] I. Dybkjær, Fuel Process. Tech. 42 (1995) 85.
[3] F. Van Looij, Ph.D. Thesis, Utrecht University, 1994.
[4] F. Van Looij, J.C. Van Giezen, E.R. Stobbe, J.W. Geus, Catal. Today 21 (1994) 495.
[5] M.S. Hoogenraad, Ph.D. Thesis, Utrecht University, 1995.
[6] P.H. Bolt, Ph.D. Thesis, Utrecht University, 1994.
[7] D. Van de Kleut, Ph.D. Thesis, Utrecht University, 1994.
[8] E. Grootendorst, Y. Verbeek, V. Ponec, J. Catal. 157 (1995) 706.
[9] W. Weimin, Y. Yongnian, Z. Jiayu, Appl. Catal. A 133 (1995) 81.
[10] Y.F. Chang, J.G. McCarty, Catal. Today 30 (1996) 163.